

Deep Learning-Based Quantization of L-Values for Gray-Coded Modulation

Marius Arvinte, Sriram Vishwanath and Ahmed H. Tewfik
Department of Electrical and Computer Engineering
University of Texas at Austin
Austin, Texas 78712
Email: arvinte@utexas.edu

Abstract—In this work, a deep learning-based quantization scheme for log-likelihood ratio (L-value) storage is introduced. We analyze the dependency between the average magnitude of different L-values from the same quadrature amplitude modulation (QAM) symbol and show they follow a consistent ordering. Based on this we design a deep autoencoder that jointly compresses and separately reconstructs each L-value, allowing the use of a weighted loss function that aims to more accurately reconstruct low magnitude inputs. Our method is shown to be competitive with state-of-the-art maximum mutual information quantization schemes, reducing the required memory footprint by a ratio of up to two and a loss of performance smaller than 0.1 dB with less than two effective bits per L-value or smaller than 0.04 dB with 2.25 effective bits. We experimentally show that our proposed method is a universal compression scheme in the sense that after training on an LDPC-coded Rayleigh fading scenario we can reuse the same network without further training on other channel models and codes while preserving the same performance benefits.

I. INTRODUCTION

Deep learning has recently gained a foothold in wireless communications and signal processing with experimental results showing that it can be used for various tasks ranging from channel code design [1] to black-box communication schemes [2]. At the same time, quantization of information in communication systems is critical for applications such as feedback channels, relay schemes or hybrid automatic repeat request storage. Motivated by finding a quantization scheme that is as greedy as possible with minimal impact to the end-to-end performance, we introduce a deep learning-based L-value vector quantization scheme that leverages a statistical ordering among them to weigh its loss function during training.

Log-likelihood ratio quantization is a well studied topic, where it has been identified that the optimal formulation aims to maximize mutual information [3]. Prior work in [4] presents a data-driven approach for quantizing L-values even in cases when the channel has an arbitrary or intractable distribution. The work in [5] introduces a maximum mutual information vector quantization method for L-values by using the Lloyd algorithm with a KL divergence metric. In both cases, a sharp drop in performance is exhibited when the effective storage size approaches or goes below two bits per L-value.

More recently, deep networks have been used for quantization and codebook learning, where the main challenge is back-propagating gradients through the quantization function.

Solutions to this include soft-to-hard approximations of the nearest neighbor function that are parameterized by an increasing attraction coefficient over time, or replacing the null gradient with other approximations. The work in [6] uses such a schedule during the training phase to learn a compression scheme for high resolution images that outperforms state-of-the-art schemes by almost an order of magnitude. With the same goal, the work in [7] introduces the architecture of vector quantized variational autoencoder (VQ-VAE) to learn a discrete, compressed representation of image and speech signals by approximating the null gradient with a linear function.

Even though these solutions are shown to be successful for images, in the case of communications the signal statistics are fundamentally different and any application requires careful analysis and design of the network architecture and loss function. Previous work in [8] uses an autoencoder structure to compress the channel state information (CSI) matrix by exploiting its time and spatial domain correlation. In this work, we propose to exploit the use of binary reflected Gray coding (BRGC), almost universally adopted in practical systems and known to be optimal [9] and show that it induces an ordering on the average magnitude of the L-values that holds for any channel coefficient distribution. We leverage this to design a deep autoencoder network that uses a branched decoder architecture to individually reconstruct each L-value, allowing us to weigh the loss function towards smaller magnitude L-values.

Our work is closest to [10], where a deep autoencoder is used to jointly compress and reconstructs the set of L-values corresponding to a channel use by leveraging the fact that three sufficient statistics will recover them. However, their work exhibits a performance gap even when the compressed signal (latent representation) is not quantized. By leveraging the statistics of L-values, we manage to virtually close this performance gap, reducing it from 0.2 dB to as low as 0.02 dB and consequently improving the quantized results as well. We compare our work with state-of-the-art maximum mutual information schemes and show that we exhibit a compression gain of up to two, allowing us to use an effective storage size of less than two bits per L-value for high order modulation schemes. Furthermore, we experimentally show that the same network weights can be used for a wide range of scenarios

with different channel models and codes, without requiring any further training or adjustments.

II. SYSTEM MODEL

Consider the digital baseband model of a binary reflected Gray coded (BRGC) M -QAM modulation scheme, where the transmitted symbol x is found by mapping the bits b_1, \dots, b_K to a complex constellation symbol belonging to the set of all constellation points C , where $K = \log_2 M$. We adopt a flat fading complex channel model in which the complex received symbol y has the expression

$$y = hx + n, \quad (1)$$

where n is drawn i.i.d. from a complex Gaussian distribution with zero mean and variance equal to $\frac{\sigma_n^2}{2}$ and h represents the complex channel coefficient. We assume that h comes from a complex distribution such that $\mathbb{E}[|h|^2] = 1$, but make no further assumptions on the shape of the distribution for the rest of our derivations. Given instantaneous channel state information at the receiver, the exact log-likelihood ratio (L-value) for bit b_k is given by

$$L_k = \log \frac{P(y|b_k=1)}{P(y|b_k=0)} = \log \left\{ \frac{\sum_{\hat{x} \in C, b_k=1} \exp -\frac{|y-h\hat{x}|^2}{\sigma_n^2}}{\sum_{\hat{x} \in C, b_k=0} \exp -\frac{|y-h\hat{x}|^2}{\sigma_n^2}} \right\}. \quad (2)$$

Prior work shows that by factoring out the h term, letting $\tilde{y} = \frac{y}{h}$ be the equalized received symbol and rewriting the expressions, the exact L-values can be reconstructed given the three sufficient statistics [10]

$$G = \left(\frac{|h|}{\sigma_n} \right)^2, \tilde{y}_r = \text{Re}\{\tilde{y}\}, \tilde{y}_i = \text{Im}\{\tilde{y}\}, \quad (3)$$

or any bijective function of them. We aim to learn such a highly nonlinear representation of these statistics with our deep network.

We further consider the conditional distributions of the L-values under the max-log approximation for different bit positions $k = 1, \dots, K$. The work in [11] shows that in a nonfading (i.e., affected only by noise) scenario the probability density function (PDF) of the L-values for each bit level can be written as a sum of truncated Gaussian PDFs. According to [11], the approximate PDF of the k -th L-value conditioned on the transmitted bit b_k has the expression

$$p_k(\lambda|b_k) = \sum_{l=0}^{\frac{M}{2}-1} w_{k,l} \Phi(\lambda; (-1)^{b_k+1} \mu_l, \sigma_l^2), \quad (4)$$

where $\Phi(\lambda; \mu, \sigma^2)$ represents the Gaussian PDF and $w_{k,l}$ is the uniform probability that L_k is a Gaussian with mean and variance given by μ_l and σ_l^2 respectively, in concordance with the Zero-Crossing Model approximation in [11]. As the authors of [11] show, this leads to a key observation about the L-values corresponding to different bit positions, namely that

after splitting the bits in two groups (due to the real/imaginary symmetry induced by BRGC) the bits occupying the first positions are more robust to channel conditions than later ones. Formally, this can be expressed by the inequality

$$\mathbb{E}[|L_1|] > \mathbb{E}[|L_2|] > \dots > \mathbb{E}[|L_{\frac{K}{2}}|], \quad (5)$$

where the expectation is taken across all noise realizations and a similar ordering holding true for the second half of L-values associated with the imaginary part. Finally, let Λ_k be the soft bit associated to the L-value L_k , given by [3]

$$\Lambda_k = \tanh \frac{L_k}{2}. \quad (6)$$

Since \tanh is a monotonic function it follows that the ordering in (5) holds for Λ_k as well. We let \mathbf{L} and $\mathbf{\Lambda}$ denote the K -dimensional real, ordered — according to (5) — vectors of L-values and soft bits corresponding to a single channel use with Λ_k and L_k their k -th elements, respectively. Our goal is to compress $\mathbf{\Lambda}$ to a three-dimensional latent representation, quantize it to a finite, small number of bits and reconstruct the original input.

The basic machine learning structure we use for compressing the L-values is a deep neural network. From a high-level perspective, a deep neural network can be viewed as a parameterized function $f(\mathbf{x}; \theta_f)$, where \mathbf{x} is the real-valued input vector and θ_f denotes the weight vector, containing the serialized weights of all layers. For the rest of this work, we only refer to feedforward, fully-connected neural networks, in which a layer that takes as input the vector \mathbf{x} and outputs \mathbf{y} implements the operation

$$\mathbf{y} = \phi(\mathbf{W}\mathbf{x} + \mathbf{b}), \quad (7)$$

where (\mathbf{W}, \mathbf{b}) represent the weights and biases associated with a layer and ϕ is the element-wise activation function and all dimensions are consistent with matrix-vector multiplication. Typical activation functions include the rectified linear unit (ReLU) given by $\phi(x) = \max\{x, 0\}$ and the hyperbolic tangent $\phi(x) = \tanh x$. Finally, an autoencoder is a deep neural network that is trained to reconstruct its own input \mathbf{x} . This is commonly achieved by performing gradient updates on the weights θ_f in order to minimize the empirical risk function

$$\mathcal{L}(\theta_f) = \frac{1}{N} \sum_{i=1}^N L(f(\mathbf{x}_i; \theta_f), \mathbf{x}_i), \quad (8)$$

where \mathbf{x}_i represents the i -th training sample and L can be chosen to any distance or quasi-distance function. Importantly, we note that gradient-based approaches are incompatible with the quantization of hidden activations in deep networks, since the gradient becomes null almost everywhere after quantization, preventing preceding weights from being updated. In this work

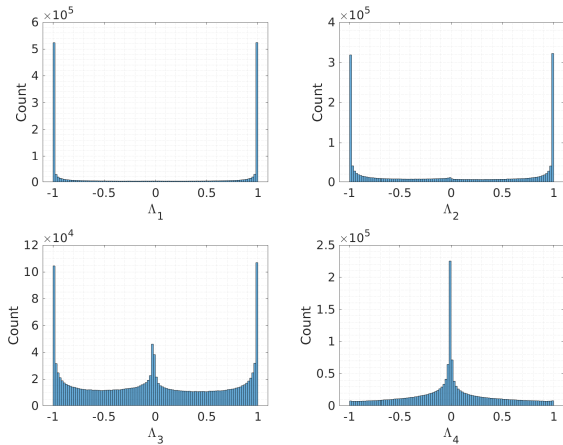


Fig. 1. Empirical PDFs for the first four soft bits of a $K = 8$ (256-QAM) transmission over a Rayleigh fading channel at 18 dB, exhibiting the ordering in (5). The next four soft bits have a similar order due to the binary reflected Gray coding.

III. THE PROPOSED SCHEME

While the original derivation is performed for a nonfading scenario, additional conditioning on the channel realization and averaging ensures the ordering of L-values holds even for an arbitrary fading distribution. We formulate and prove the following proposition.

Proposition 1: The ordering in (5) holds for any arbitrary distribution of h .

Proof: First we note that by (3) knowledge of $|h|^2$ is sufficient to characterize the distribution of L-values, since the phase can always be corrected assuming full CSI is available. By letting $g = |h|^2$ and expanding the PDF of the k -th L-value we obtain

$$p_k(\lambda|b_k) = \int_0^\infty p_k(\lambda|b_k, g) f_g(g) dg, \quad (9)$$

where f_g is the PDF of g . Considering $p_k(\lambda|b_k, g)$, it follows that (4) holds for any fixed g , thus the ordering (5) holds pointwise, thus it holds globally. ■

The previous result is proven for the max-log approximation of the L-values, but empirically holds for the complete expression as well. In the case of a fading channel Fig. 1 illustrates this property by plotting four of the eight distributions of the soft bits for a 256-QAM scenario, where it can be clearly observed that the latter bits have much lower average reliability than the earlier ones. This asymmetry of the different bit locations has wide implications in forward error correction coding scenarios, especially in the mid-high signal-to-noise ratio regime, where accurate reconstruction of low L-values is shown to be critical for correct decoding [12].

This key observation motivates the architecture of our compression and reconstruction network. Since we target vector quantization of the set of all L-values corresponding for a channel use, accurate reconstruction of the latter bit locations is crucial for high order modulation, otherwise a

simple averaged error (e.g., the very common mean squared error) will not capture high relative errors on low values. Furthermore, this reconstruction property is also desirable in the soft bit domain, since the hyperbolic tangent function is approximately linear around the origin.

To achieve our goal, we propose an autoencoder with a *branched decoder* that employs one separate deep network to reconstruct each input channel. The architecture of our solution is shown in Fig. 2. The network takes as input the vector of soft bits Λ and feeds them to the encoder, where the compressed latent representation \mathbf{z} is output. Letting $f(\cdot; \theta_f)$ be the encoder part of the network and $g_k(\cdot; \theta_{g_k})$ each of the bit decoders, the k -th reconstructed soft bit can be expressed as

$$\tilde{\Lambda}_k = g_k(\mathbf{z}; \theta_{g_k}) = g_k(f(\Lambda; \theta_f); \theta_{g_k}). \quad (10)$$

Since prior work successfully uses a latent representation \mathbf{z} of dimension three equal to the number of sufficient statistics in (3), we adopt the same model here and set $\mathbf{z} \in \mathbb{R}^3$.

To account for accurate reconstruction of low magnitude soft bits, we adopt two measures:

- 1) We use a sample-wise weighted mean squared error function as in [10]. The loss function between the k -th soft bits and its reconstruction has the expression

$$L(\tilde{\Lambda}_k, \Lambda_k) = \frac{|\tilde{\Lambda}_k - \Lambda_k|^2}{|\Lambda_k| + \epsilon}, \quad (11)$$

where $\epsilon = 10^{-6}$ is used for numerical stability. This formulation ensures that more importance is given to soft bits with low values in the same bit location.

- 2) We use a set of real weights $w_k \geq 0$ to weigh the contributions of each soft bit to the total loss function leading to the expression

$$\mathcal{L}(\tilde{\Lambda}, \Lambda) = \sum_{k=1}^K w_k \sum_{i=1}^N L(\tilde{\Lambda}_k^{(i)}, \Lambda_k^{(i)}), \quad (12)$$

where the weights are normalized to satisfy $\sum_k w_k = 1$, thus at least one weight must be positive.

Note that the weights w_k are not applied per sample, but rather per soft bit and ensure that more importance is placed on reconstructing certain bit positions. By using Proposition 1 and the ordering in (5), we order the weights w_k in decreasing order of reliability by

$$w_1 \leq w_2 \leq \dots \leq w_{\frac{K}{2}}, \quad (13)$$

$$w_{\frac{K}{2}+1} \leq w_{\frac{K}{2}+2} \leq \dots \leq w_K.$$

Once the weights are set, the architecture is jointly trained for a number of epochs. Since we are using a single encoder, all gradient updates are averaged (with the weights w_k factored in) and θ_f is updated, while θ_{g_k} are individually updated for each of the constituent decoders. We note that a different training regime is also possible, where only the weights of specific decoders are updated if the performance after joint training

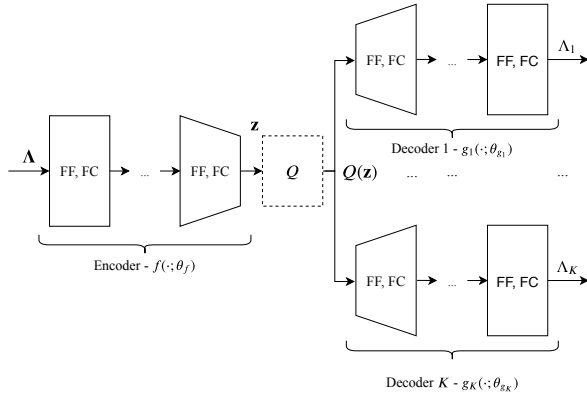


Fig. 2. Block diagram of our proposed deep network architecture with one decoder for each soft bit. Each solid rectangular box represents a feedforward, fully-connected layer. The dashed block represents the latent representation quantizer and is not active during training.

is not good enough on specific soft bits. In fact, the scheme is completely modular in terms of the decoders, meaning that we can replace any of them with other reconstruction methods once the encoder is fixed.

Once training is complete, we have a universal, compressed representation of the soft bits in the form of \mathbf{z} and the next step is quantizing and storing the latent representation. Letting $\hat{\mathbf{z}}_i, i = 1, \dots, 2^{N_b}$ be the N_b -bit codebook in the latent space the quantization function is given by

$$Q(\mathbf{z}) = \underset{\hat{\mathbf{z}}}{\operatorname{argmin}} \|\mathbf{z} - \hat{\mathbf{z}}\|_2. \quad (14)$$

The use of a minimum distortion quantization in the latent space is justified by prior work showing that overparametrized deep networks are naturally robust to quantization of their activations [13]. Finally, reconstruction is performed by applying the decoders for each soft bit on the quantized latent representation $\hat{\mathbf{z}}$.

IV. PERFORMANCE RESULTS

A. Architectural and Training Details

We use a number of three hidden layers for the encoder and each of the decoders, with a uniform intermediate output size of $4 \times K$, except for the latent representation which has a dimension of three as discussed in Section III. Storing weights in 32-bit floating precision leads to a total memory footprint (considering the quantization codebook negligible) lower than 83 KB for $K = 8$ (256-QAM), and scaling on the order of K^2 , thus rapidly decreasing for lower order modulations.

All hidden activations are ReLU, except for the latent representation and the outputs, which come from tanh. During training, we also add a small amount of additive white Gaussian noise with zero mean and $\sigma_t = 10^{-3}$ to the latent representation before it is decoded to encourage generalization and robustness to numerical quantization. Since the latent representation \mathbf{z} comes from a \tanh activation, this bounds each of its elements to $[-1, 1]$ and avoids learning trivial

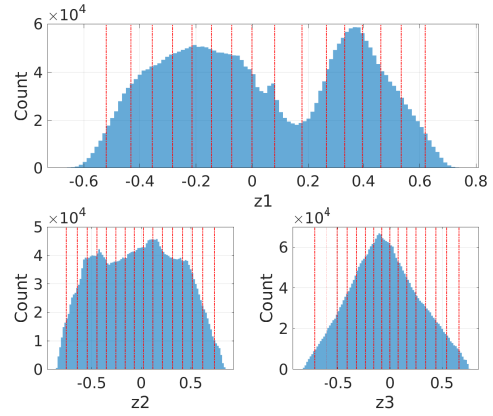


Fig. 3. Histograms of the three components of \mathbf{z} after training and the resulted one-dimensional k-Means quantization codebooks with 4 bits (16 levels) per latent component in dashed red lines. The Cartesian product of these quantizers is used to derive the Q function. This latent representation is only trained once and reused for different channel models and codes.

solutions such as boosting the power of \mathbf{z} to overcome the added noise.

We use the Adam algorithm for minimizing the empirical risk function in (12) with a batch size of 65 536 samples, learning rate of 0.001 and recommended parameters [14] and split the training in two phases. The entire procedure is summarized in Algorithm 1. In the first phase the encoder and all decoders are jointly trained starting with equal weights $w_k = \frac{1}{K}$. After a number of epochs N_{e_1} the average reconstruction error e_k is computed for all soft bits in the training data and we update the weights w_k as

$$w_k = \frac{e_k}{\sum_{i=1}^K e_i}. \quad (15)$$

This process is repeated for a number of rounds N_r , placing a higher importance on soft bits that have larger average reconstruction errors. We empirically observe that this procedure always respects the order induced by (13) and also converges to a steady state where the weights no longer need an update. Alternatively, if a closed form expression of the distribution of $p_k(\lambda|b_k)$ is available and can be numerically evaluated one can use a fixed set of weights inversely proportional to $\mathbb{E}[|L_k|]$.

In the second phase we freeze the weights of the encoder and continue individual training for each decoder for a number of $N_{e_{2,k}}$ epochs. Here we leverage the branched architecture to improve the performance of individual decoders without affecting the learned representation. We explore options where $N_{e_{2,k}}$ is equal or proportional to the stationary w_k , but both cases lead to roughly the same performance. Since each decoder only updates its own weights, this process is fully parallelizable among them.

Once training is completed, we apply a mini-batch version of the k-Means algorithm [15] to independently obtain a non-uniform scalar quantizer for each of the three components of the latent representation. Note that this has the advantage of

Algorithm 1: Training procedure

Data: $\Lambda_i \in \mathbb{R}^K, i = 1, \dots, N$.
Randomly initialize weights θ_f, θ_{g_k} .
Initialize weights $w_k = \frac{1}{K}, \forall k = 1, \dots, K$.
Stage 1. Encoder and decoders jointly optimized.
for $i = 1$ to N_r **do**
 Train with fixed w_k for a number of N_{e_1} epochs.
 for $j = 1$ to N_{e_1} **do**
 Mini-batch Adam update of weighted loss function.
 for $b = 1$ to N_b **do**
 $\theta_f, \theta_{g_k} \leftarrow \text{Adam}(\Lambda_i, w_k, \theta_f, \theta_{g_k})$
 end
 end
 Compute average reconstruction error for each L-value.

$$e_k = \frac{1}{N} \sum_{i=1}^N L(\tilde{\Lambda}_i, \Lambda_i)$$

 Update weights using (15).
end
Stage 2. Individual decoder training.
for $k = 1$ to K **do**
 for $i = 1$ to $N_{e_{2,k}}$ **do**
 Mini-batch Adam update of loss function.
 $\theta_{g_k} \leftarrow \text{Adam}(\mathbf{z}_i, \theta_{g_k})$
 end
end

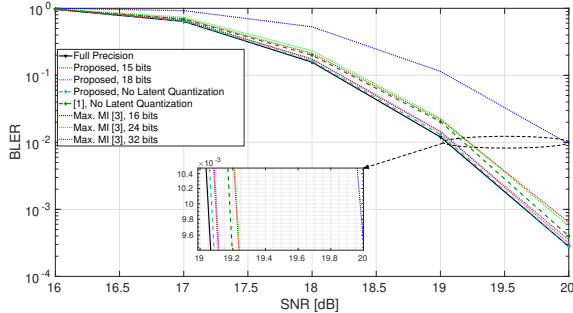


Fig. 4. BLER performance of the proposed quantization scheme in a Rayleigh fading scenario with LDPC coding and $K = 8$ (256-QAM) modulation.

drastically minimizing the storage requirements of the codebook versus vector quantization of the latent space and is also empirically observed to offer similar or better performance. The training data consists of L-values computed using (2) and generated from the coded bits of a number of 10 000 LDPC codewords with a length of 648 and rate 1/2 transmitted over a Rayleigh fading channel with $h \sim \mathcal{CN}(0, 1)$. The complete source code, pretrained networks and all performance results are available online¹.

B. Impact of Quantization on Block Error Rate

Throughout this section, we show the results obtained for $K = 8$ (256-QAM), but the architecture can be readily used for any modulation scheme. Since the number of quantized values is a constant w.r.t. K , the scheme offers more efficient compression for high-order modulation schemes. The first experiment involves investigating the performance of our scheme in the same conditions in which the training data is generated. We generate 10 000 LDPC codewords for each signal-to-noise ratio in the set $\{16, 17, 18, 19\}$ dB, corresponding to a high-mid noise power regime, concatenate the data points and shuffle them. Once training is completed, we design the k-Means quantizers using the latent representation of the same dataset. The empirical marginal distributions of the three components of \mathbf{z} are shown in Fig. 3 together with their quantization codebooks. For validation, we generate a set of unseen 100 000 LDPC codewords across a slightly wider signal-to-ratio range, encode them, quantize the latent representation with the trained codebooks and reconstruct them, followed by LDPC decoding using belief propagation with 50 iterations.

We compare the performance of our method with the maximum mutual information quantization in [4], where we train a reference quantization for each separate bit position to account for large order modulation schemes, as well as use an initial codebook constrained in the $[-3, 3]$ to further boost performance. Additionally, we include the full precision (unquantized latent representation) results from [10] to show that we successfully cover the performance gap coming from the autoencoder reconstruction. Fig. 4 shows the obtained block error rate (BLER) curves for all the schemes, as well as the unquantized performance. Comparing at BLER = 0.01 we notice that we achieve the same performance with 15 bits instead of 24, leading to a compression ratio of 1.6 times and a loss of performance smaller than 0.2 dB when compared to full precision storage, while using an equivalent of $\frac{15}{K} = 1.875$ bits per L-value. As a contrast, using the scheme in [4] with 2 bits per L-value leads to a performance loss of almost 1 dB.

C. Generalization Performance

We now investigate the performance of the proposed quantization scheme when applied to different configurations than the one we train on. Fig. 5 shows the validation performance of the network trained in Section IV-B when the channel is a frequency domain representation of a multitap fading ETU channel, corresponding to an OFDM scenario. Each LDPC codeword experiences a different realization of the ETU channel and we use a random, but fixed interleaver for extra robustness. We point out that the BLER performance is fully preserved when quantizing to 15 or 18 bits, even though the network and codebooks are not further trained or adjusted in any way for this particular scenario.

Additionally, we investigate the performance of the same network when applied to a Polar-coded Rayleigh fading scenario. We simulate a polar code of length 256 and rate 1/2

¹<https://github.com/mariusarvinte/deep-llr-quantization>

V. CONCLUSIONS

In this work we have introduced a universal log-likelihood ratio (L-value) compression and quantization method that uses a deep autoencoder with a branched decoder, quantizes and reconstructs the latent representation of all L-values corresponding to a channel use. The branched decoder architecture allows us to more accurately reconstruct low-magnitude L-values, which are critical for successful decoding under greedy quantization.

Our results show that we can afford quantization with less than two effective bits per L-value for 256-QAM modulation, regardless of the type of channel model or code used with a loss smaller than 0.1 dB in terms of BLER. In the high performance regime, we achieve losses smaller than 0.05 dB with an effective 2.25 bits per L-value. The algorithm can be used for any modulation scheme (with better gains achieved for higher order schemes) and is competitive with state-of-the-art maximum mutual information quantization algorithms, achieving a compression factor of up to 1.8 times for the same accuracy.

REFERENCES

- [1] H. Kim, Y. Jiang, S. Kannan, S. Oh, and P. Viswanath, "Deepcode: Feedback codes via deep learning," in *Advances in Neural Information Processing Systems*, 2018, pp. 9436–9446.
- [2] T. O'Shea and J. Hoydis, "An introduction to deep learning for the physical layer," *IEEE Transactions on Cognitive Communications and Networking*, vol. 3, no. 4, pp. 563–575, 2017.
- [3] W. Rave, "Quantization of log-likelihood ratios to maximize mutual information," *IEEE Signal Processing Letters*, vol. 16, no. 4, pp. 283–286, 2009.
- [4] A. Winkelbauer and G. Matz, "On quantization of log-likelihood ratios for maximum mutual information," in *2015 IEEE 16th International Workshop on Signal Processing Advances in Wireless Communications (SPAWC)*. IEEE, 2015, pp. 316–320.
- [5] M. Danieli, S. Forchhammer, J. D. Andersen, L. P. Christensen, and S. S. Christensen, "Maximum mutual information vector quantization of log-likelihood ratios for memory efficient harq implementations," in *2010 Data Compression Conference*. IEEE, 2010, pp. 30–39.
- [6] E. Agustsson, F. Mentzer, M. Tschannen, L. Cavigelli, R. Timofte, L. Benini, and L. V. Gool, "Soft-to-hard vector quantization for end-to-end learning compressible representations," in *Advances in Neural Information Processing Systems*, 2017, pp. 1141–1151.
- [7] A. van den Oord, O. Vinyals *et al.*, "Neural discrete representation learning," in *Advances in Neural Information Processing Systems*, 2017, pp. 6306–6315.
- [8] C. Lu, W. Xu, H. Shen, J. Zhu, and K. Wang, "Mimo channel information feedback using deep recurrent network," *IEEE Communications Letters*, vol. 23, no. 1, pp. 188–191, 2018.
- [9] E. Agrell, J. Lassing, E. G. Strom, and T. Ottosson, "Gray coding for multilevel constellations in gaussian noise," *IEEE Transactions on Information Theory*, vol. 53, no. 1, pp. 224–235, 2006.
- [10] M. Arvinte, A. H. Tewfik, and S. Vishwanath, "Deep log-likelihood ratio quantization," *Accepted for Publication at EUSIPCO '19*, 2019. [Online]. Available: <http://arxiv.org/abs/1903.04656>
- [11] A. Alvarado, L. Szczecinski, R. Feick, and L. Ahumada, "Distribution of l-values in gray-mapped m 2-qam: Closed-form approximations and applications," *IEEE Transactions on Communications*, vol. 57, no. 7, pp. 2071–2079, 2009.
- [12] X. Zhang and P. H. Siegel, "Quantized iterative message passing decoders with low error floor for ldpc codes," *IEEE Transactions on Communications*, vol. 62, no. 1, pp. 1–14, 2013.
- [13] Y. Guo, "A survey on methods and theories of quantized neural networks," *arXiv preprint arXiv:1808.04752*, 2018.
- [14] D. P. Kingma and J. Ba, "Adam: A method for stochastic optimization," *arXiv preprint arXiv:1412.6980*, 2014.

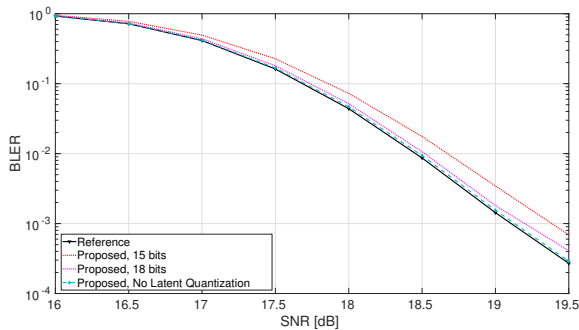


Fig. 5. BLER performance of the proposed quantization scheme in a ETU fading scenario with LDPC coding and $K = 8$ (256-QAM) modulation. The same network and codebooks used in Fig. 4 are reused without additional training or adjustments.

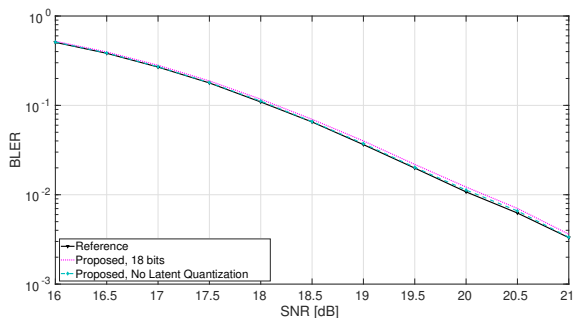


Fig. 6. BLER performance of the proposed quantization scheme in a Rayleigh fading scenario with Polar coding and $K = 8$ (256-QAM) modulation. The same network and codebooks used in Fig. 4 are reused without additional training or adjustments.

used for the NR control channels. Fig. 6 plots the BLER performance on 100 000 codewords obtained with the same network, where we can notice that greedy quantization causes the same small losses. This leads us to the claim that the learned quantization scheme is universal, in the sense that it exhibits the same performance regardless of the type of channel or channel code used and does not require any further training whatsoever.

D. Discussion

The performance of our scheme can be further extended if we take into account that we are not forced to keep the resolution of all latent space components equal. Indeed, judging by Fig. 3 it may appear that the second component z_2 is more sensitive to scalar quantization since its distribution has a higher entropy. Thus, given a budget of 16 bits, we expect that allocating them to (z_1, z_2, z_3) as $(5, 6, 5)$ instead of, say, $(5, 5, 6)$ produces better quality results. Due to space constraints and to not make the figures too crowded we omit this result, but this is indeed the case. This reasoning can be further extended to groups of latent components if vector quantization is applied in the latent space, but we leave this for future research.

- [15] D. Sculley, "Web-scale k-means clustering," in *Proceedings of the 19th international conference on World wide web*. ACM, 2010, pp. 1177–1178.